Supporting Information

for Energy Environ. Sci., Cite this: DOI: 10.1039/x0xx00000x

Dopant–Free Polymeric Hole Transport Material for Highly Efficient and Stable Perovskite Solar Cells

Guan-Woo Kim[a‡], Gyeongho Kang[a‡], Jinseck Kim[b], Gang-Young Lee[a], Hong Il Kim[a], Limok Pyeon[a] and Jaechol Lee[b], Taiho Park[a*]

[*] Prof. Taiho Park. Corresponding-Author
[‡] There authors are contributed equally to this manuscript.

[a] *Pohang University of Science and Technology (POSTECH), 77 Cheongam-Ro, Nam-gu, Pohang, Kyoungbuk, Korea. Fax: +82-54-279-8298; Tel: 82-54-279-2394; E-mail: taihopark@postech.ac.kr*

[b] *Future Technology Research Center, Corporate R&D, LG Chem Research Park, 188, Moonji-ro, Yuseong-gu, Daejeon, 34122, Republic of Korea. Tel: +82-42-870-6818*

Contents

Table S2. Efficiency tables in various device configurations.

Table S3. Summary of hysteresis in tin oxide (SnO_2) planar device employing **RCP, RCP** (ADDs), and spiro-MeOTAD (ADDs).

Experimental details

a) Synthesis of RCP, P-R, and P-OR

RCP was prepared in the inert condition by mixing 2,6-bis(trimethyltin)-4,8-bis(2-ethylhexyl-2-thenyl)-benzo[1,2-b:4,5-b′]dithiophene (1g, 1.105mmol), 4,7-bis(5-bromo-4-dodecylthiophen-2-yl)-2,1,3-benzothiadiazole (0.439g, 0.553mmol), 4,7-bis(5-bromothiophen-2-yl)-5,6-bis(dodecyloxy)benzo[c][1,2,5] thiadiazole (0.457g, 0.553mmol, tris(dibenzylideneacetone) dipalladium(0) (2 mol%), and tri(o-tolyl)phosphine (8 mol%) into 15 mL chlorobenzene in a 20 mL microwave vial. The polymerization was under the reaction by heating at 120 °C for 5 min, at 140 °C for 5 min, and at 170 °C for 60 min in a microwave reactor. The polymer was end-capped by addition of 2-tributylstannylthiophene and the mixture was further reacted at 140 °C for 20 min. The solution was cooled down and 2-bromothiophene was added by syringe, and the mixture was heated at 140 °C for another 20 min. After the reaction was finished, the crude polymer was precipitated into the methanol and further purified by soxhlet extraction with acetone, hexane, and chloroform. The extracted polymer in chloroform was precipitated into methanol, filtered, and dried under vacuum. **P-R** was prepared in the same way, mixing 2,6-bis(trimethyltin)-4,8-bis(2-ethylhexyl-2-thenyl)-benzo[1,2-b:4,5-b′]dithiophene (0.5 g, 0.553 mol) and 4,7-bis(5-bromo-4-dodecylthiophen-2-yl)-2,1,3-benzothiadiazole (0.439 g, 0.553 mol). **P-OR** was prepared in the same way, mixing 2,6-bis(trimethyltin)-4,8-bis(2-ethylhexyl-2-thenyl)-benzo[1,2-b:4,5-b′]dithiophene (0.5 g, 0.553 mol) and 4,7-bis(5-bromothiophen-2-yl)-5,6-bis(dodecyloxy)benzo[c][1,2,5] thiadiazole (0.457 g, 0.553 mol). Nuclear magnetic resonance (NMR) was measured to identify each polymer (Fig. S1), but the signals were too broad to be distinguished from the baseline because each of polymers was large and rigid.[1] The molecular weights (M_n) of **RCP**, **P-OR**, and **P-R** are 26,700 (PDI = 1.96), 21,000 (PDI = 2.30), and 20,000 (PDI = 2.22), respectively (See Fig. S1). In addition, all polymers generally exhibited amorphous characteristics as seen in Fig. S2.

b) Synthesis of a $CH_3NH_3PbI_3$ perovskite

The $CH_3NH_3PbI_3$ perovskite was synthesized as already reported. First, CH_3NH_3I was synthesized by reacting 27.86 mL methylamine (40 wt% in methanol, Junsei Chemical Co.) and 30 mL hydroiodic acid (57 wt% in water, Aldrich) in a round-bottomed flask at 0 °C for 2 h with stirring. The resulting materials were obtained by evaporation and recrystallization and finally dried at 60 °C in a vacuum oven overnight. PbI_2 was purchased from Aldrich. The $CH_3NH_3PbI_3$ perovskite was obtained using sequential deposition (dipping) method.

c) Solar cell fabrication

Perovskite solar cells were fabricated on fluorine-doped tin oxide (FTO) coated glass substrates. The FTO coated glass substrates were etched using zinc powder and 2M hydrochloric acid (HCl). Then, they were rinsed with detergent, deionized water (DI water), acetone, and isopropyl alcohol (IPA), successively, and then dried overnight. Tin oxide (SnO_2)

compact layer solution (0.1128g $SnCl_2 \cdot 2H_2O$ in 5 mL ethanol) is spin-coated at 2000 rpm for 60 s on the UV-ozone treated substrates, forming ~50 nm layer. SnO_2 compact layer is annealed at 200 °C for 30 min. Perovskite layer was introduced using sequential deposition method. PbI_2 solution (462 mg/mL in dimethylformamide) is spin-coated at 2000 rpm for 30 s and dried in the air. Resulting PbI_2 layer is dipped in MAI solution (10 mg/mL in isopropyl alcohol) for 8 min, and finally forms black perovskite. Perovskite is annealed at 70 °C for 30 min. Hole transport material solutions (**1**: 72.3 mg spiro-MeOTAD with 27.8 μL tBP, 17.8 μL LiTFSI (520 mg/mL in acetonitrile), and 1 mL chlorobenzene, **2**: 15 mg **RCP** with 1 mL chlorobenzene, **3**: 15 mg **RCP** with 20.4 μL tBP, 20.4 μL LiTFSI (28.3 mg/mL in acetonitrile), and 1 mL chlorobenzene) were spin-coated at 5000 rpm for 30 s. Finally, gold electrode (100 nm) was thermally evaporated in high vacuum condition.

d) Device characterization

Using a Keithley 2400 SMU and an Oriel xenon lamp (450 W) with an AM1.5 filter, the solar cells were characterized in air under AM 1.5G illumination of 100 mW cm^{-2} (Oriel 1 kW solar simulator), which was calibrated with a KG5 filter certified by NREL. After light soaking for 1 minute, the current density-voltage (J-V) curves of all devices were measured by 0.15 V/s of scan rate with 200 ms voltage settling time. The active area of device is 0.09 cm^2.

e) SCLC measurement

Space charge limited current was measured to obtain hole mobility of RCP, P-OR, and P-R. PEDOT:PSS (Clevios P, VP AI 4083) was spin-coated on the cleaned indium tin oxide (ITO) substrate at 5000 rpm for 30 sec and then annealed at 140 °C for 10 min. The polymer solution (15 mg/mL in chlorobenzene) was spin-coated at 3000 rpm for 30 sec on the substrate. After drying, gold electrode (100 nm) was thermally evaporated in high vacuum condition.

f) IPCE measurement

The IPCE spectra were measured under a constant white light bias of approximately 5 mW/cm^2 supplied by an array of white light emitting diodes using a power source with a monochromator (Zahner GmbH) and a multimeter and chopped at approximately 5 Hz.

g) Time resolved photoluminescence measurements

Time resolved photoluminescence measurements were performed using time correlated single photon counting (TCSPC) system (HAMAMATSU/C11367-31). For TCSPC measurements, a pulsed laser source was laser diode with a wavelength of 474 nm, a repetition rate of 100 kHz, fluence of ~ 4 nJ cm^{-2} and a pulse width of 70 ps. In this study, an excitation wavelength of 474 nm and an emission wavelength of 770 nm were used. The samples were excited from the glass side under ambient conditions.

h) Stability test

Various sets of devices were kept in two conditions: 1) low humidity (dry condition, 25%), 2) high humidity (humid condition, 75%) The humidity was strictly controlled using precise hygrometer. The devices were periodically measured.

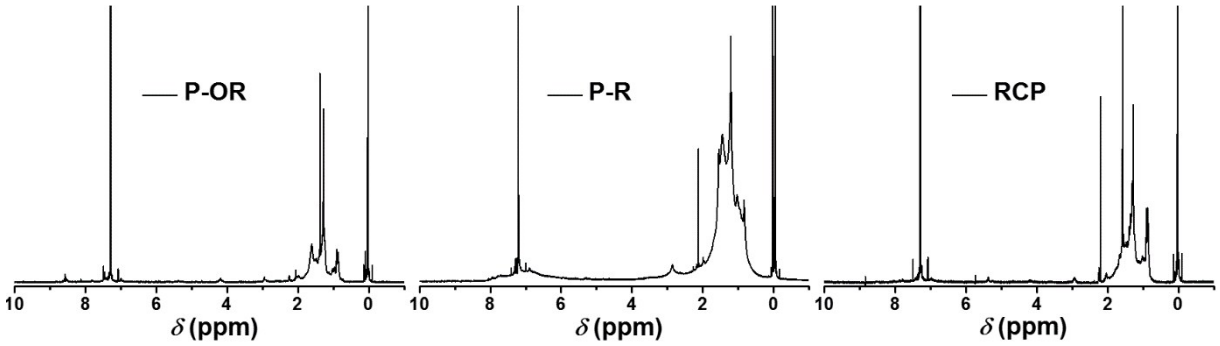

Fig. S1 500 MHz ^{1}H NMR spectra of **P-OR**, **P-R**, and **RCP.**

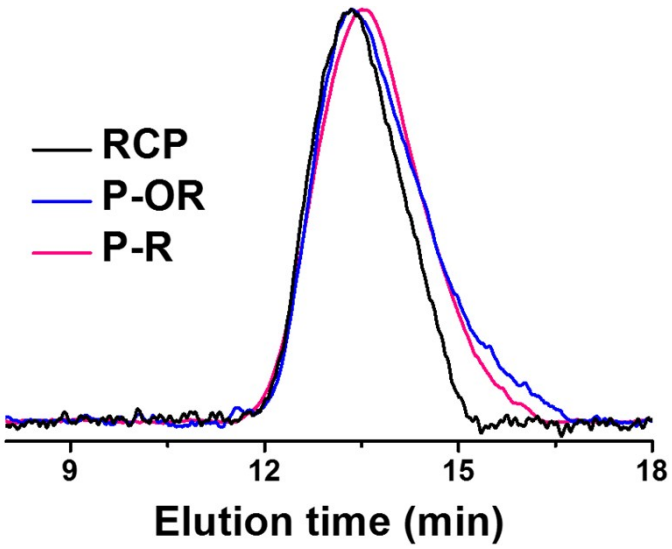

Fig. S2 Gel permeation chromatography (GPC) analysis for **P-OR**, **P-R**, and **RCP.**

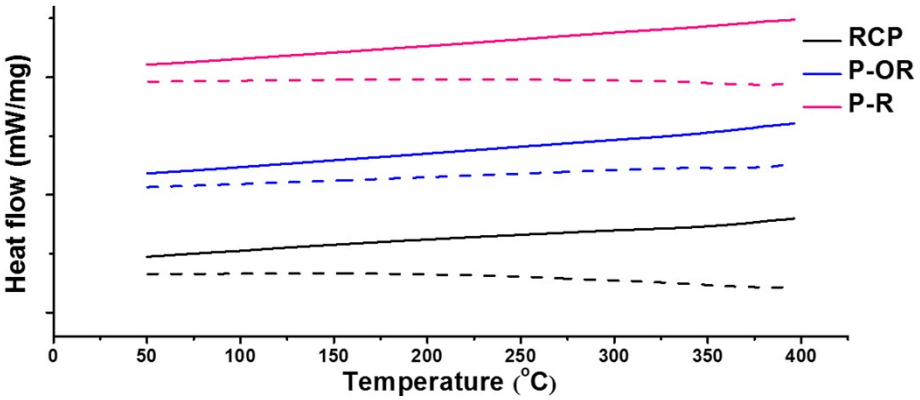

Fig. S3 Differential scanning calorimetry (DSC) of **P-OR**, **P-R**, and **RCP.**

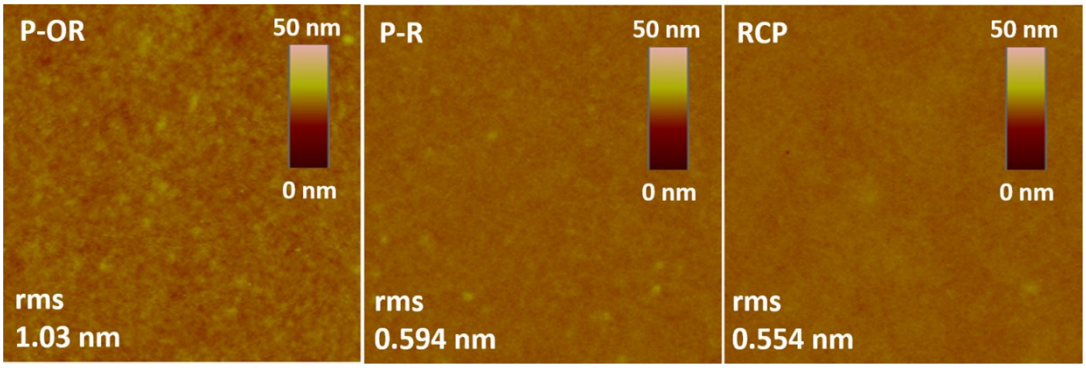

Fig. S4 Atomic force microscope (AFM) images of **P-OR**, **P-R**, and **RCP.**

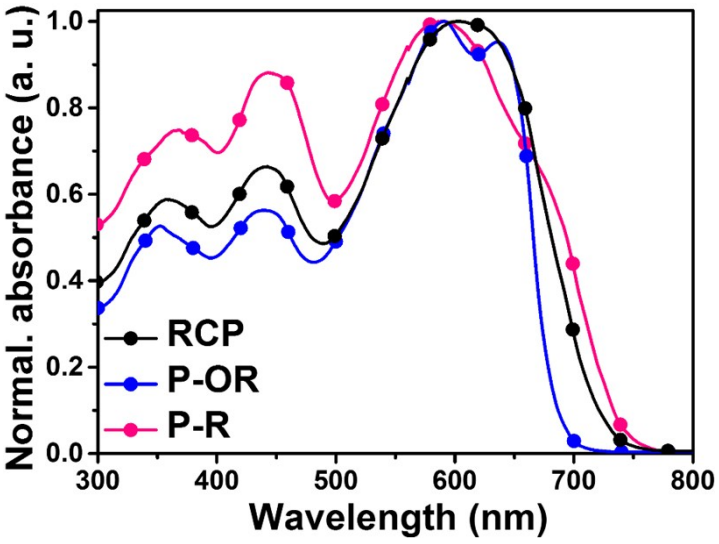

Fig. S5 UV-Vis. Absorption spectra of **P-OR**, **P-R**, and **RCP.**

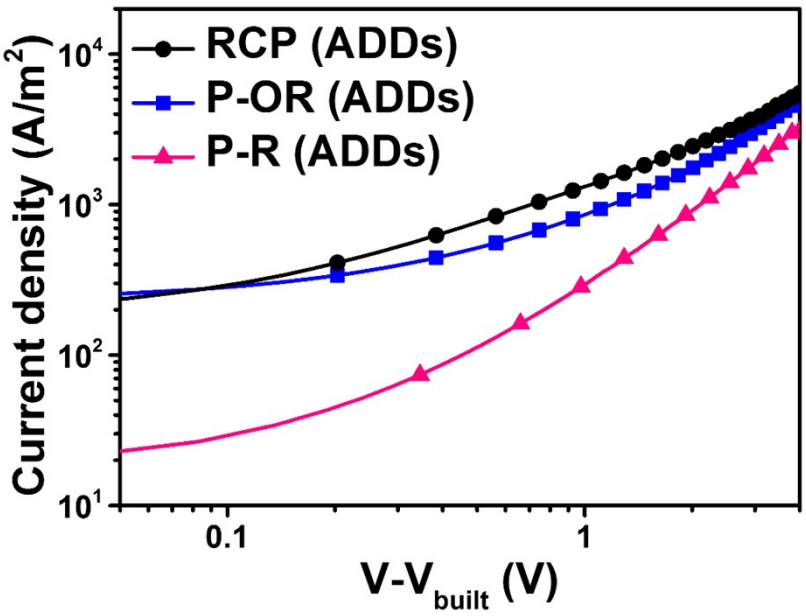

Fig. S6 Space charge limited current curves for **P-OR**, **P-R**, and **RCP** in the presence of dopants.

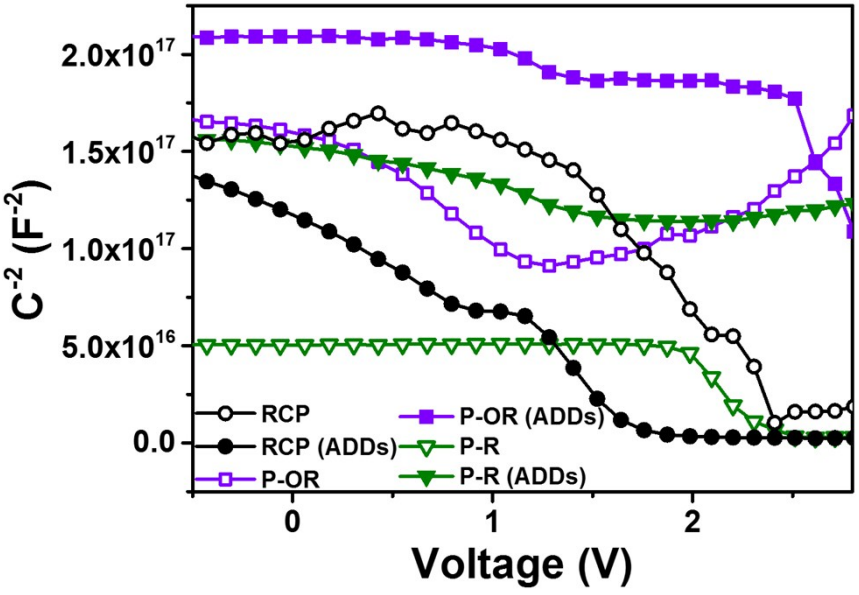

Fig. S7 Mott-Schottky analysis for **P-OR**, **P-R**, and **RCP** in the presence or absence of dopants.

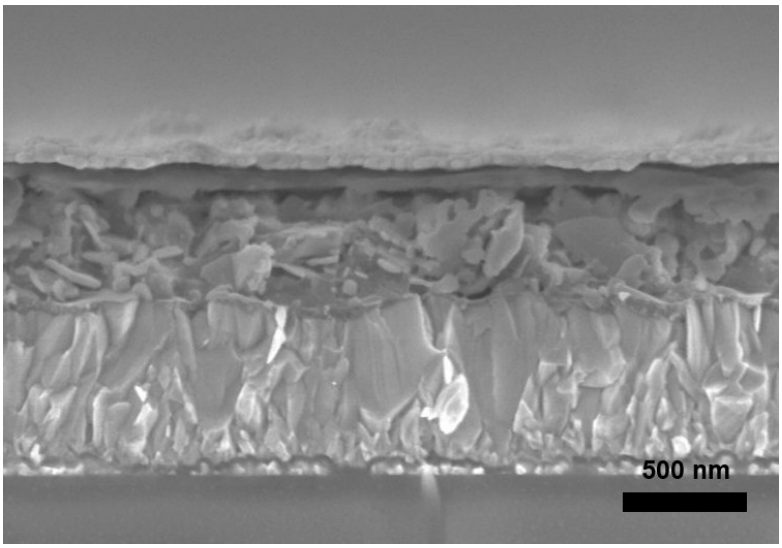

Fig. S8 Cross-sectional scanning electron microscopy (SEM) image of the device with additives.

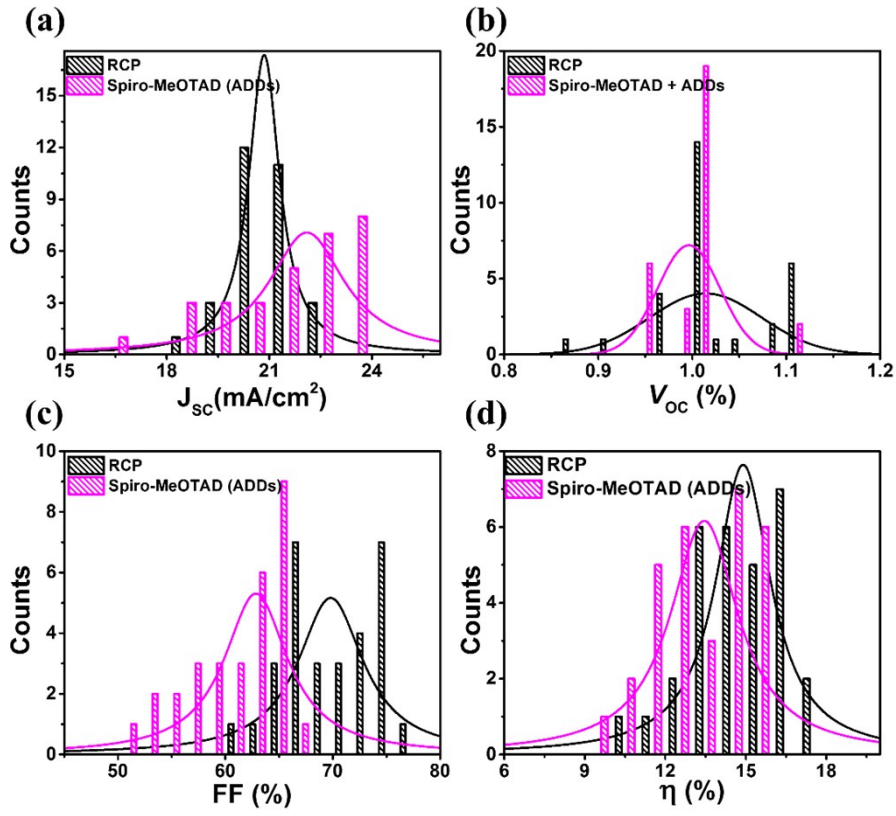

Fig. S9 Photovoltaic parameters histograms for **RCP** and spiro-MeOTAD in the presence of dopants: (a) J_{SC}, (b) V_{OC}, (c) FF, and (d) PCE.

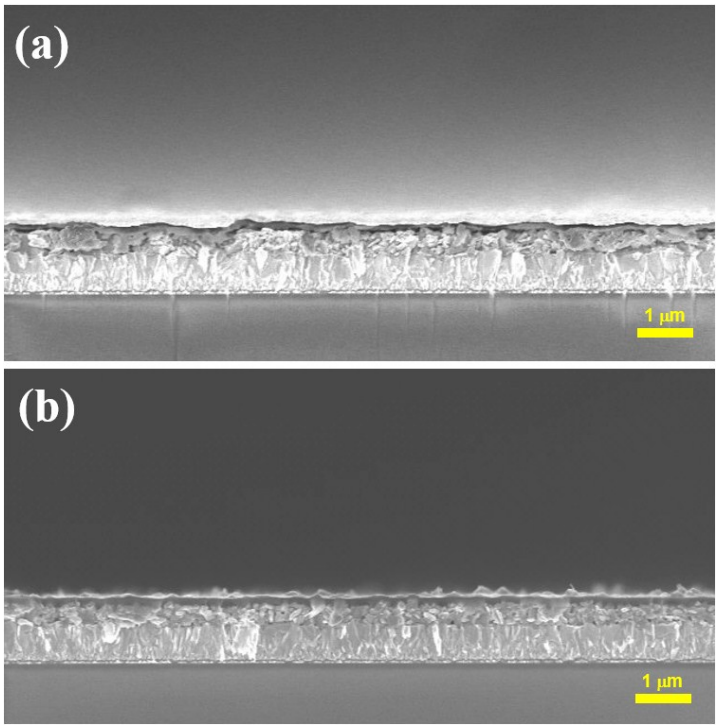

Fig. S10 Cross-sectional scanning electron microscope (SEM) images of (a) device employing **RCP** and (b) device employing spiro-MeOTAD in the presence of dopants.

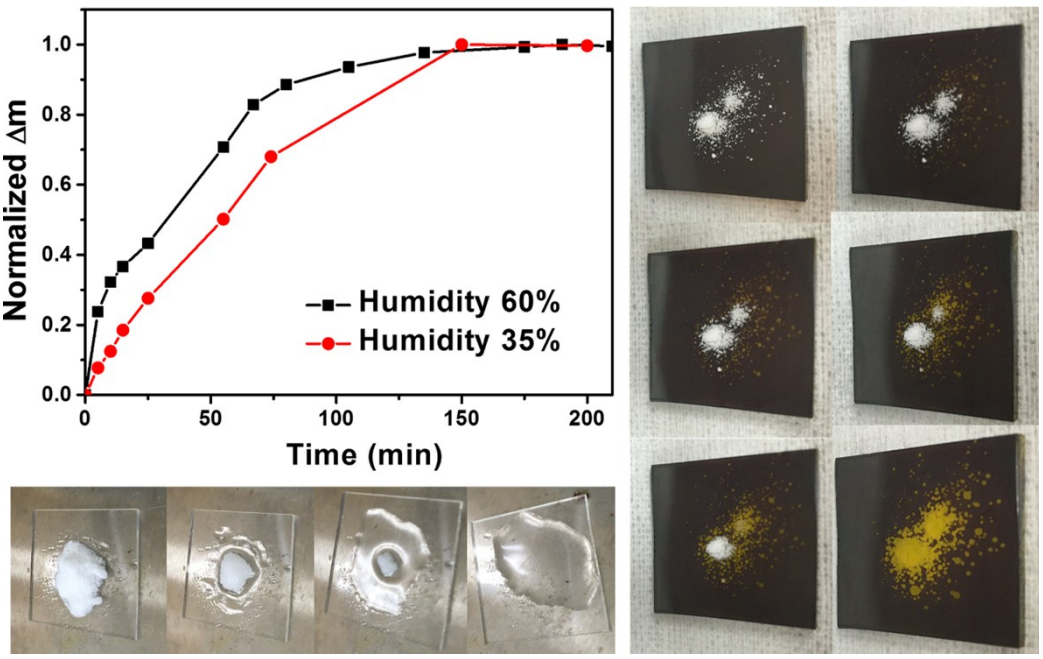

Fig. S11 Deliquescent characteristics of lithium bis(trifluoromethanesulfonyl)imide (LiTFSI): deliquescent speed, absorbing the moisture in the air and detrimental effect on perovskite film.

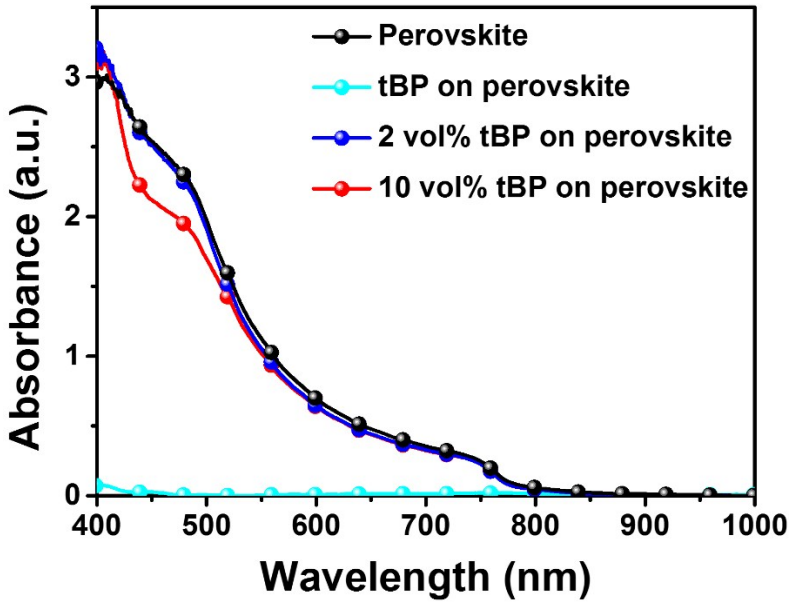

Fig. S12 The effect of tert-butylpyridine (tBP) on the absorbance of perovskite films.

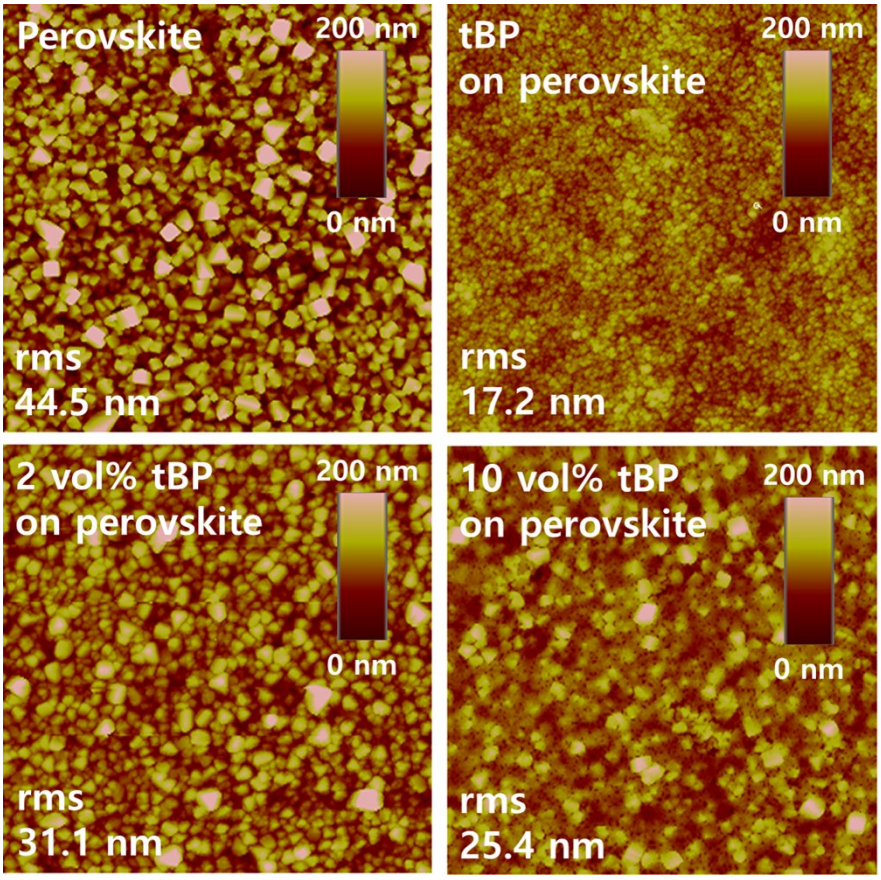

Fig. S13 AFM images of perovskite film and tBP-coated perovskite film by changing the concentration of tBP.

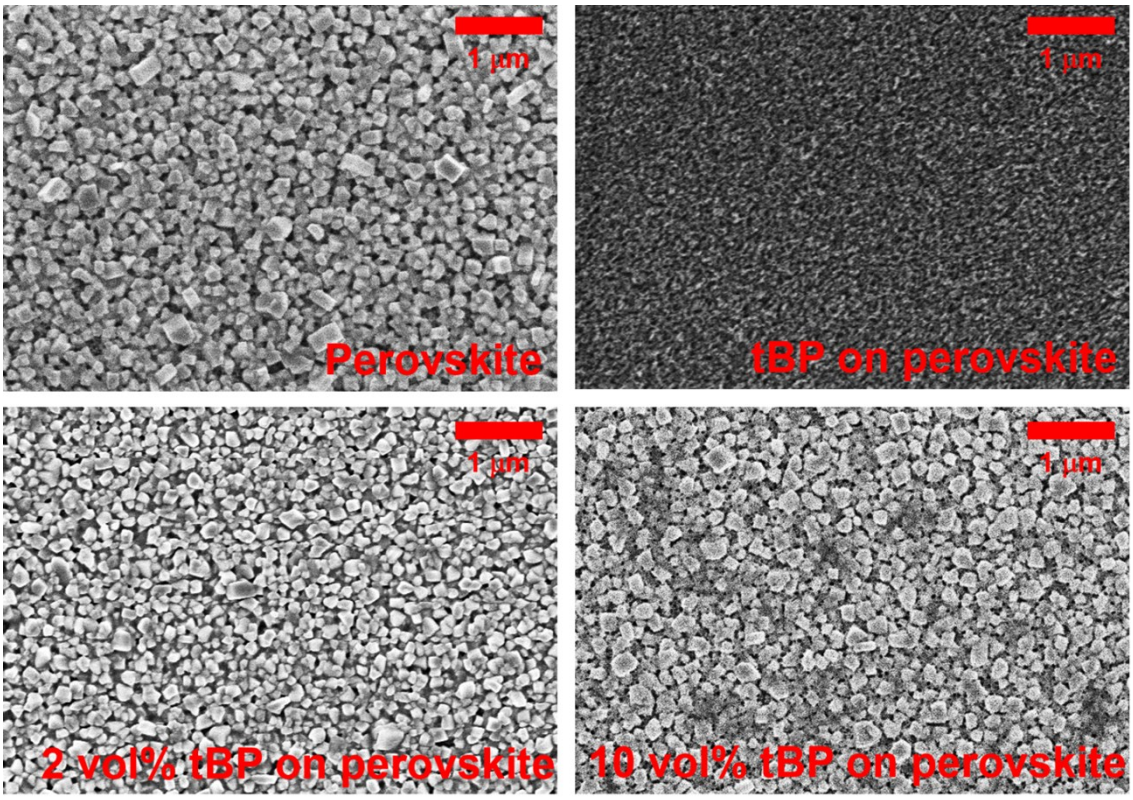

Fig. S14 SEM images of perovskite film and tBP-coated perovskite film by changing the concentration of tBP.

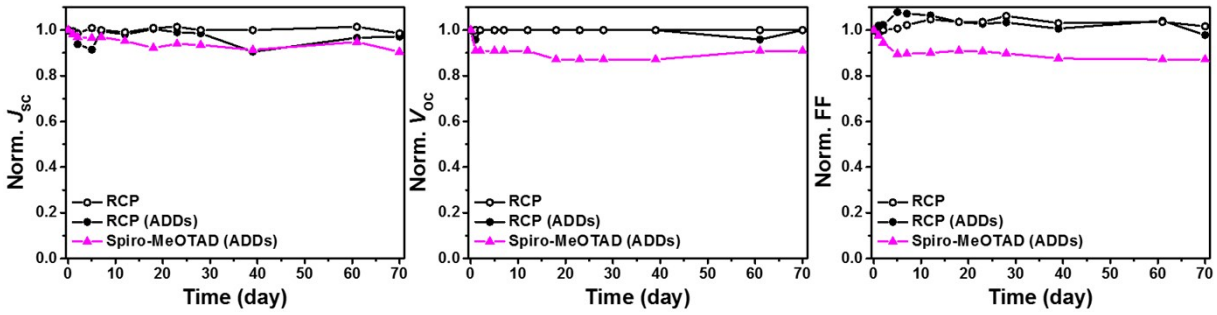

Fig. S15 Photovoltaic parameters changes of devices employing **RCP**, **RCP** in the presence of dopants, and spiro-MeOTAD in the presence of dopants under 25% of humidity.

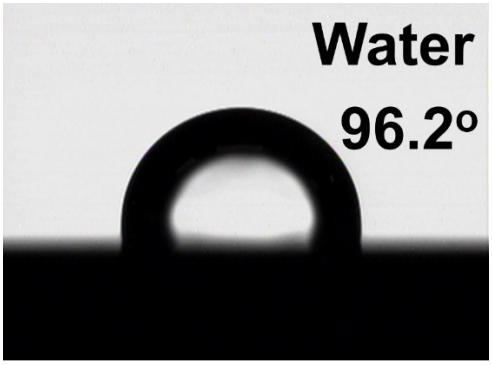

Fig. S16 Water contact angle of **RCP** to show hydrophobicity.

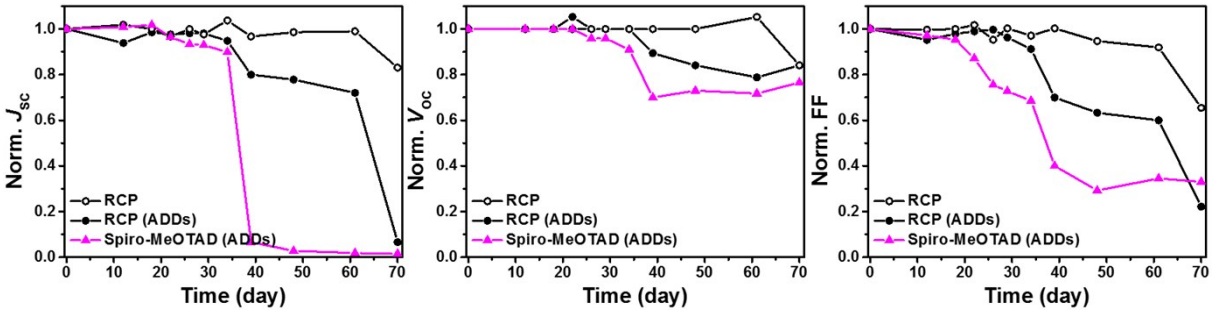

Fig. S17 Photovoltaic parameters changes of devices employing **RCP**, **RCP** in the presence of dopants, and spiro-MeOTAD in the presence of dopants under 75% of humidity.

Table S1. Summary of effective carrier density for **P-OR**, **P-R**, and **RCP** in the presence or absence of dopants.

	Effective carrier density[a] **(cm^{-3})**
P-OR	1.32×10^{16}
P-OR (ADDs)	3.53×10^{16}
P-R	1.67×10^{16}
P-R (ADDs)	2.99×10^{16}
RCP	5.97×10^{15}
RCP (ADDs)	1.10×10^{16}

[a] effective carrier density was obtained from Mott-Schottky analysis in the configuration of ITO/polymer/Al at high frequency (100 kHz): $N = \frac{-2\Delta V}{q\varepsilon_0\varepsilon_r A^2 \Delta(1/C^2)}$, where N is the carrier density and A is the device area.[2, 3]

Table S2. Efficiency tables in various device configurations.

Device configuration		J_{SC} (mA/cm^2)	V_{OC} (V)	FF (%)	PCE (%)
After optimization	FTO/SnO_2/$MAPbI_3$/**RCP**/Au	21.9	1.08	75.0	17.3
	FTO/SnO_2/$MAPbI_3$/**RCP** (ADDs[a])/Au	22.2	1.04	70.2	16.5
1st trial	FTO/SnO_2/$MAPbI_3$/**RCP**/Au	21.4	1.02	66.7	14.4
	FTO/SnO_2/$MAPbI_3$/**RCP** (ADDs)/Au	21.6	1.02	64.2	13.9
FTO/bl-TiO_2/m-TiO_2/$MAPbI_3$/**RCP**/Au		21.3	0.96	64.8	13.3
FTO/bl-TiO_2/m-TiO_2/$MAPbI_3$/**RCP** (ADDs)/Au		16.3	0.96	67.8	10.6
FTO/TiO_2/Al_2O_3/$MAPbI_3$/**RCP**/Ag		19.3	0.94	52.6	9.5
FTO/TiO_2/Al_2O_3/$MAPbI_3$/**RCP** (ADDs)/Ag		19.6	0.82	66.3	10.7

[a] ADDs: LiTFSI (2 mM) + tBP (0.07 mM)

Table S3. Summary of hysteresis in tin oxide (SnO_2) planar device employing **RCP, RCP** (ADDs[a]), and spiro-MeOTAD (ADDs).

	Scan direction	J_{SC} (mA/cm^2)	V_{OC} (V)	FF (%)	PCE (%)
RCP	Reverse	21.9	1.08	75.0	17.3
RCP	Forward	20.6	1.00	60.8	12.6
RCP (ADDs)	Reverse	22.3	1.05	70.2	16.5
RCP (ADDs)	Forward	21.0	1.00	59.3	12.5
Spiro (ADDs)	Reverse	22.9	1.01	66.4	15.3
Spiro (ADDs)	Forward	23.2	0.959	55.8	12.4

[a] ADDs: LiTFSI (2 mM) + tBP (0.07 mM)

Reference

1. M. H. Rahman, H.-L. Chen, S.-A. Chen and P. P. J. Chu, *J. Chin. Chem. Soc.*, 2010, **57**, 490-495.

2. Y. S. Lee, J. H. Park and J. S. Choi, *Opt. Mater.*, 2002, **21**, 433-437.

3. M. Zhu, T. Cui and K. Varahramyan, *Microelectronic Engineering*, 2004, **75**, 269-274.